6. Flugel, G., *Forsch. Gebiete Ingenieurw., Forschungsheft,* 395 (1939); *Natl. Advisory Comm. Aeronaut. Tech. Mem* 982 (1941).
7. Forstall, W., and A. H. Shapiro, *J. App. Mech.,* 17, 399 (1950).
8. Keenan, J. H., et al., *J. App. Mech.,* 17, 299 (1950).
9. Kivnick, A., *Eng. Expt. Sta. Univ. Illinois Tech. Rept.* 2, DA-18-064-CML-445 (1952).
10. Kroll, H. E., *Chem. Eng. Progr.,* 43, 21 (1947).
11. Ledgett, L. A., Preprint, Am. Soc. Mech. Engrs., Summer Meeting (1934), George Reproduction Co. (1934).
12. McElroy, G. E., *U. S. Bur. Mines Tech. Paper* 678 (1945).
13. Reichardt, H., *Z. Math. u. Mech.,* 21, 257 (1941).
14. Reid, E. G., *Natl Advisory Comm. Aero Tech. Note* 1949 (1949).
15. Viktoren, K., *Forsch. Gebiete Ingenieurw.* 12, 1, 16 (1941); *Natl. Advisory Comm. Aeronaut. Tech. Mem.* 1096 (1946).

III. Correlation of Profiles of Total Momentum and Energy Flux in a Nonisothermal Jet Discharging into a Duct

The data in the first paper of this series on the distribution of momentum and energy in nonisothermal air streams mixing in a straight duct were correlated by the methods described in the second paper. Mixing indexes were evaluated and used to correlate profiles of total momentum and stagnation temperature at various sections of the duct.

The understanding and prediction of the processes that take place when a fluid stream mixes turbulently with another of different velocity, composition, or temperature is becoming of ever greater technological importance. This paper studies the mixing of a round jet of heated air, discharged into a straight, cylindrical duct, with a freely induced ambient air stream. The *mixing index,* a quantity which is a measure of the degree to which the two streams remain unmixed at any given section of flow, was computed from the experimental data presented in the first paper of this series and was correlated theoretically by methods described in the second. From this correlation, empirical spreading coefficients were evaluated, and these were used to predict distribution of energy and momentum flux (temperature and velocity distribution) at various sections.

APPARATUS AND PROCEDURE

The aparatus and procedure employed in the experimental work, the results of which are correlated here, have been described in detail in Part I of this series. All the data were obtained at an air-flow rate of 2.07 std. cu. ft./sec., as metered through a calibrated orifice. The air was heated to 222° to 225°F. as measured upstream from the flow nozzle.

RESULTS

Correlation of the Mixing Index for Momentum Transport. On approach to the problem of correlating the momentum data it was clear that account would have to be taken of the scatter in the integral mass flux noted in connection with Figure 14 of Part I. This scatter is amplified in momentum-flux calculations, where the velocity enters as the square, and to an even greater extent in mixing-index calculations, where the velocity enters as the fourth power. It was noticed that the individual points on the velocity profiles did not show much scatter relative to one another and that the continuous curves appeared to be reasonably well defined. It seemed to be more likely that the scatter in the integral mass flux resulted from random changes of 5 to 10% in the flow pattern and induction ratio between successive profile measurements. This effect has been noticed by others(*3*) and is thought to reflect a true physical instability in the system.

It was postulated, however, that the relative shape of a momentum-flux profile, rather than its relative position, is the true measure of the degree of mixing of the two streams, and it seemed reasonable that some method of normalizing the profiles might eliminate the scatter and yield reliable values of the mixing index. Implicit in this is the hypothesis that the mixing is a function only of the geometry of the system and independent of the relative velocities of the initial streams. The manner in which the generalized flux function M was constructed [Equation (7)*] accomplishes the desired normalization as shown by the fact that it leads to an analytical solution [Equations (20) and (25) and discussion] that is independent of the relative velocities, provided the spreading coefficient c is independent also. Although this in general is probably not the case(*2*), minor variations in the flow ratio, as encountered here, should result in only second-order variations in c.

In Part II the necessity of evaluating m_∞ at each cross section because of the unavoidable loss of momentum at the wall of the duct was discussed [Equation (41)]. The

*All equations referred to appear in Part II.

present scatter is an effect of the same kind but of a larger order of magnitude and may be treated in the same way.

The following procedure was used in assigning values to $m_{j,avg}$ and $m_{i,avg}$ appearing in Equation (7). The first profile was taken at 1 in. from the nozzle. It was assumed that the velocity on the axis of flow here was the same as at the nozzle discharge. A value of 20,500 ft.-lb./(sec.) (sq.ft.)/sec. was calculated for $m_{j,avg}$ from the impact and static pressure data for this profile, as it was assumed that this value fairly represented the average momentum flux density over the nozzle discharge. It is possible by use of this value of $m_{j,avg}$ and $m_{\infty,x}$ as defined by Equation (41) to calculate by difference an apparent $m_{i,avg}$ at each cross section by use of Equation (27). The results are shown in Table 1.

TABLE 1

x, distance from nozzle, in.	$m_{i\ avg.}$, ft. lb./(sec.)/(sq. ft.) sec.
1	396
4	95
7	480
10	291
16	—98
20	131
23	171
26	96

It is seen that there is considerable variation, and in one instance a negative value occurred. Reference to Equation (33) shows that the stream momenta enter into the calculation of the mixing index as the term $(m_{j,avg}-m_{i,avg})^2$. Although $m_{i,avg}$ is small compared with $m_{j,avg}$, nevertheless, when the difference is squared, the variations in $m_{i,avg}$ introduce fluctuations into the gamma values. But it is these fluctuations which it is desired to eliminate by the normalization procedure.

The quantity $m_{i,avg}$ may be estimated in another way. The static pressure at the first profile was —2.6 in. of water relative to the atmosphere. If the inlet section of the duct is treated as an ideal-flow nozzle, it is readily calculated that the flow momentum, $\overline{\rho u^2}$, is 896 ft. lb./(sec.)/(sq.ft.)/sec. Conversion of the static pressure to momentum units gives P_g equal to —436. The sum, which is the total momentum of the induced stream, m_i, is 433, which is in fair agreement with the value listed in Table 1 for the first profile. Since there was undoubtedly some irreversibility in the flow in the inlet section of the duct, it was decided to use a compromise value of 400 for $m_{i,avg}$ throughout the calculations.

The mixing index γ was evaluated at the various cross sections by graphical integration of Equation (33). The values listed in Table 2 when plotted vs. x defined a smooth curve which appeared to extrapolate with reasonable probability to a gamma of 0.165. This is the theoretical value at x equal to zero for the system studied as calculated from Equation (40) with nozzle diameter d of 0.898 in. and duct diameter D of 3.81 in. The spreading coefficient c was then evaluated by the method discussed in Part II [Equation (49)] and found to be 0.0480. Values of the mixing-index ratio γ/γ_o are listed in Table 2 and are shown plotted in Figure 1. The solid curve represents Equation (39) with b taken as zero. This value of b correlates the data better than any positive value. In fact, the three points at highest cx/D lie below the curve, implying that the mixing here is proceeding more rapidly than corresponds to b equal to zero. The correlation could be improved by increasing the mixing coefficient c and taking negative values of b. Physically this situation would correspond to the condition where the presence of the duct wall increases the rate of growth of Λ over that occurring in free jets. Such a possibility cannot be excluded because the boundary layer at the wall does generate turbulence; however, as discussed in Part II, the correlation is not sensitive to variations in b, and the scatter in the present data prevents a precise evaluation of b. For this reason, the data were provisionally correlated with b taken as zero.

The correlation in Figure 1 is reasonably good. A correlation of momentum data obtained with an isothermal jet in the same apparatus used in this study has been published elsewhere(*1*). In that case, c was found to be 0.0445. It appears that heating the jet to 225°F. may have increased the rate of mixing of the two streams compared with the isothermal case. However, sufficient data have not been accumulated to permit estimating the precision of these values of c, and it would be premature to conclude that heating the jet affected the mixing significantly.

Correlation of the Mixing Index for Energy Transport. Mixing indexes were calculated from the temperature and momentum data of Part I by means of Equations (56), (7), and (33). It was observed that the temperature profile taken nearest the discharge of the nozzle did not have a central region of uniform temperature corresponding to the core of uniform velocity observed in the momentum measurements. Although no temperature profile in the nozzle discharge was obtained, it is readily apparent that it could not have been uniform because of heat losses to the nozzle and antecedent piping. However the relative nonuniformity was certainly not great—at most 5° or 6°F. It was believed that the equations devel-

TABLE 2.—EXPERIMENTAL VALUES OF MIXING INDEX FOR MOMENTUM TRANSPORT

$\frac{x}{D}$	$\frac{x}{d}$	γ	γ/γ_o	$\frac{cx}{D}$ ($c=0.0480$)
0.00	0.00	(0.165)	(1.000)	0.000
0.26	1.11	0.140	0.849	0.013
1.05	4.45	0.102	0.618	0.050
1.84	7.80	0.0754	0.457	0.088
2.62	11.1	0.0470	0.285	0.126
4.20	17.8	0.0126	0.076	0.202
5.25	22.3	0.0056	0.034	0.252
6.03	25.6	0.0021	0.013	0.290
6.83	29.0	0.0007	0.004	0.328

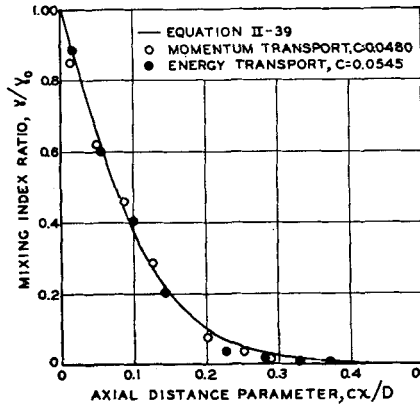

FIG. 1. CORRELATION OF MIXING-INDEX RATIO FOR MOMENTUM AND ENERGY TRANSPORT.

oped in Part II on the basis of an assumed uniformity of initial jet temperature could be used with reasonable success in correlating the data and that marked discrepancies would appear only adjacent to the nozzle. The mean energy flux, $m_{\infty,x}$, was calculated from Equation (41), and the results are listed in Table 3.

TABLE 3.—EXPERIMENTAL VALUES OF MIXING INDEX FOR ENERGY TRANSPORT

$\frac{x}{D}$	$\frac{x}{d}$	$m_{\infty,x}$	γ	γ/γ_o	$\frac{cx/D}{(c=0.0545)}$
0.00	0.00	...	(0.165)	(1.000)	0.000
0.26	1.11	240	0.1459	0.884	0.014
1.05	4.45	269	0.0991	0.601	0.057
1.84	7.80	267	0.0663	0.402	0.100
2.62	11.1	240	0.0330	0.200	0.143
4.20	17.8	206	0.0060	0.036	0.229
5.26	22.3	235	0.0026	0.016	0.286
6.03	25.6	240	0.0010	0.006	0.329
6.83	29.0	246	0.0005	0.003	0.372

Considerable scatter is observed in the values of $m_{\infty,x}$. These should show only a monotonic decrease with increasing x owing to loss of heat at the wall. The average of these values gave 4,460 for $m_{j,avg}$ when substituted into Equation (27). This value was used throughout the calculations. The resulting values of γ when plotted vs. x defined a smooth curve which could be extrapolated with reasonable probability to 0.165. The gammas were then normalized with respect to $\gamma_o = 0.165$ and the spreading coefficient c was evaluated by Equation (49). A value of 0.0545 was obtained. The mixing-index ratios γ/γ_o are listed in Table 3 and are plotted in Figure 1. The scatter appears to be of the same order as that for the momentum transfer data, and the same trend to values less than theoretical with increase in cx/D is observed.

As the spreading function Λ is proportional to c^2, the ratio of the lambdas for energy and momentum transport may be evaluated:

$$\frac{\Lambda_E}{\Lambda} = \frac{C_E^2}{c^2} = \left(\frac{0.0545}{0.0480}\right)^2 \cong 4/3 \qquad (1)$$

which is in agreement with the hypothesis introduced in Part II.

Prediction of Energy- and Momentum-Flux Profiles in the Ducted Jet. Theoretical values of M, which may represent either momentum- or energy-flux density in the theory used here, were calculated from Equation (21) with d/D equal to 0.236. They are listed in Table 4† as a function of r_* with cx/D as the parameter and are plotted in Figure 2 vs. cx/D with r_* as parameter. Profiles of M at any cx/D may be obtained from that figure.

† For Tables 4, 5, and 6 (III D-F) order document 4485 from American Documentation Institute, Auxiliary Publications Service, Library of Congress, Washington 25, D. C., remitting $1.75 for microfilm or $2.50 for photoprints.

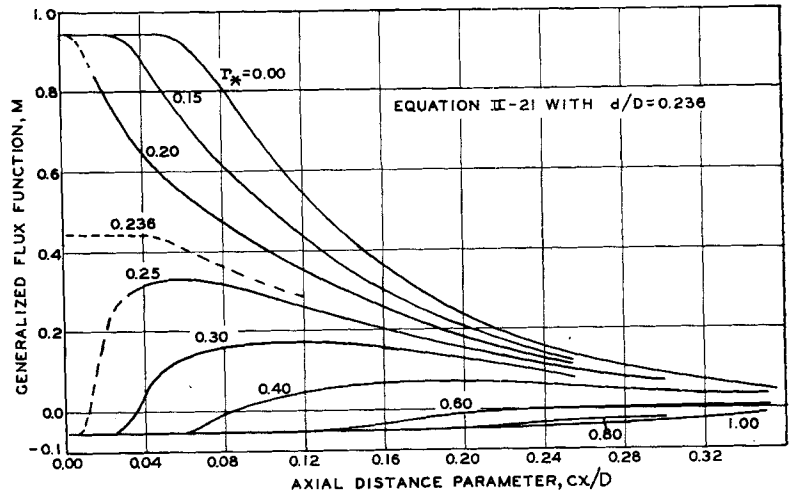

FIG. 2. GENERALIZED FLUX FUNCTION.

Only twenty terms of the series in Equation (21) were used. The series converges very slowly for r equal to d/D. Scatter was observed in calculated M at r_* values of 0.20 and 0.25, being greater in the latter case. However, it is believed that the best smooth curve through the points is sufficiently reliable for present purposes and that the uncertainty involved is within the probable error in the experimental data.

Correlation of the Generalized Flux Function M for Simultaneous Transport of Energy and Momentum. The function M of Equation (7) was calculated from the momentum-flux data. The same values of m_j and m_i were used as in the calculation of the mixing indexes. The results are listed in Table 5† and are plotted in Figure 3. Also shown as solid lines are curves taken from Figure 2 at the appropriate values of x/D, and with c equal to 0.0480 as evaluated from the mixing-index correlation. It is seen that the agreement is within the precision required for engineering calculations. The curve at x/D of 0.26 shows the data to fall off as r_* approaches unity. This is believed to be indicative of a tendency toward separation of the flow in the vicinity of the sharply rounded entrance plate. In subsequent curves only the point nearest the wall shows appreciable diminution; this is thought to signify the presence of a thin boundary layer.

As expected from the trend exhibited by the gamma correlation, the M correlation shows the points along the center line to lie above the theoretical curve close to the nozzle and below the curve farther away.

In a similar way, the data on the distribution of energy were correlated. The M values are listed in Table 6† and are plotted in Figure 4, together with solid curves cross-plotted from Figure 2. The initial temperature profile in the jet stream was not uniform because of experimental difficulties. As a result, the central points on the curve at x/D of 0.262 lie above the theoretical curve, as expected. On

the other hand, it is unlikely that the nonuniformity of the initial jet temperature can account for the excessive magnitudes of the M values near the center of the profile at x/D of 1.84 and 2.62. This is more probably the same effect noted in the momentum-flux correlation and represents a fundamental defect in the theory.

under one set of operating conditions, and it is not known how the spreading coefficients vary with the ratios of velocities, diameters, and temperatures of the jet and induced streams. The transport variables were defined in such a way that, if the theory is correct, the spreading coefficient should be independent of diameter and temperature ratio. The theory provides no clue concerning the dependence of the spreading coefficient on the velocity ratio. The system used in these experiments is intermediate between the extremes of a free jet discharging into a stagnant fluid and a jet discharging into a stream having nearly the same velocity. The evidence is that the spreading coefficient varies from 0.075 for free jets down to zero as the velocity ratio approaches unity (*2*).

SUMMARY AND CONCLUSIONS

The data on turbulent transport of momentum and energy presented in Part I may be successfully correlated by the method developed in Part II. The correlation depends upon the evaluation of two empirical coefficients, c and b. However it is insensitive to variations in b, which is a measure of the limitation imposed by the duct on the growth of the scale of the turbulence. A value of zero for b was found to be not inconsistent with the data. Thus momentum- and energy-flux profiles were correlated in effect by the single (spreading) coefficient c, the value of which was 0.0480 for momentum transport and 0.0545 for energy transport. The theory neglected radial static pressure gradients as well as momentum and heat losses at the wall of the duct; neverthe-

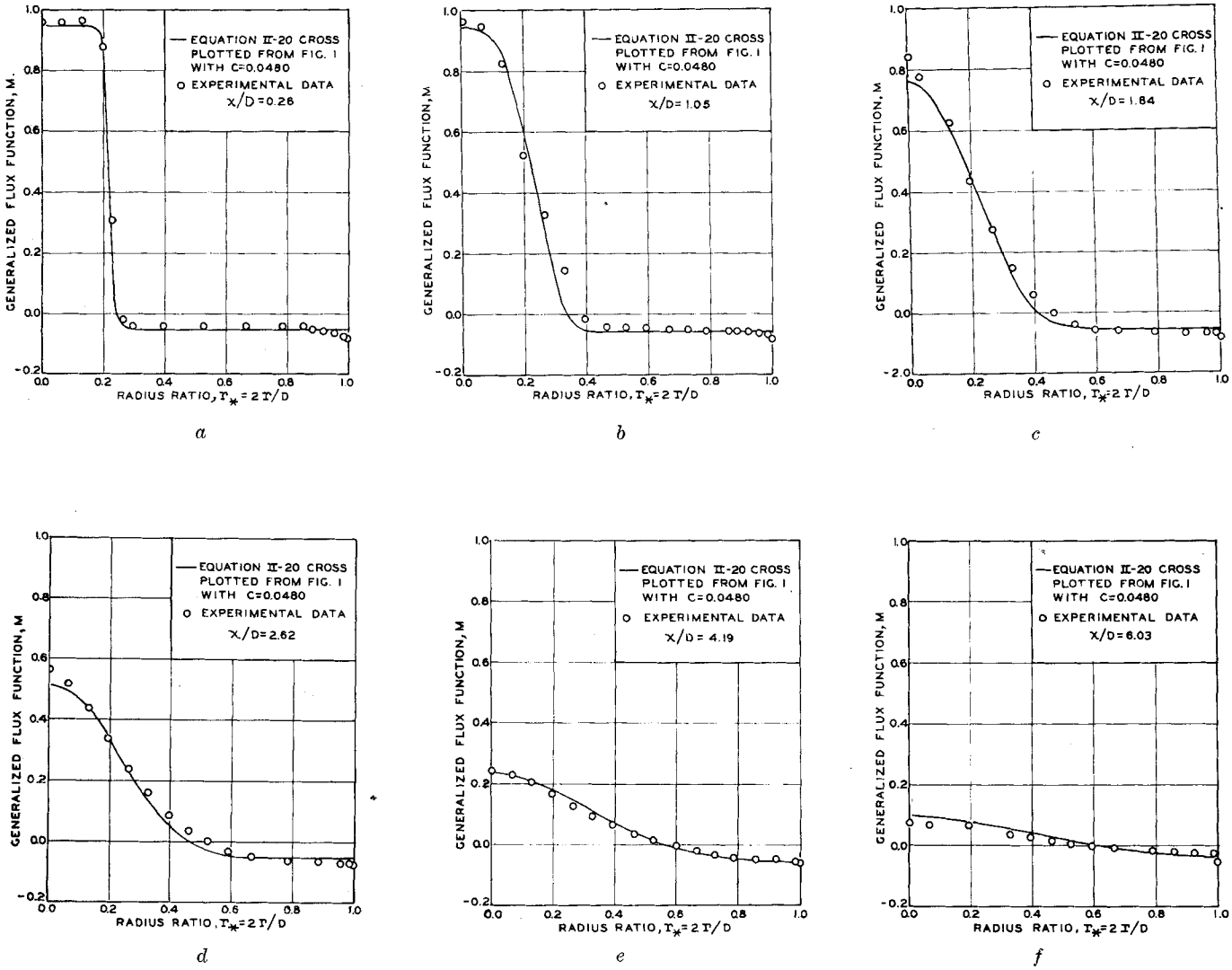

FIG. 3. CORRELATION OF GENERALIZED FLUX FUNCTION M FOR MOMENTUM TRANSPORT.

As before, at increasing x/D, the experimental points tend to fall below the theoretical curves, whether because of neglect of heat loss at the wall or of some other defect in the theory is uncertain. The M curves could all be rectified by progressive diminution of the corresponding m_j's. However very precise data yielding values of m with negligible scatter would be required for such a procedure to be feasible.

The experiments were performed

less these values of c suffice to describe satisfactorily the entire flow field.

ACKNOWLEDGMENT

The comments and suggestions of H. F. Johnstone, E. W. Comings, and Clarke Coldren are gratefully acknowledged. This study was performed as a part of a program of the Engineering Experiment Station, University of Illinois, under Contract N6-ori-71, T. O. XI, sponsored jointly by the Office of Naval Research and Flight Research Laboratory.

NOTATION

b = empirical coefficient in Equation (19), a measure of the effect of the duct wall on the growth of the scale of the turbulence

c = momentum spreading coefficient, empirical coefficient in Equation (19)

D = diameter of mixing duct

d = diameter of jet nozzle

M = variable defined by Equation (7); M is proportional to the flux density of total momentum or of energy as the case may be

m = flux density of total momentum or of energy, Equation (8), Equation (69)

P_g = gauge static pressure in duct. $\bar{P} - P_{atm}$.

r_* = normalized radial coordinate, $r_* = 2r/D$

u = x-directed component of velocity

x = axial coordinate, distance along axis of duct from nozzle

Greek

γ = mixing index, Equation (33)

Λ = proportionality function in Reichardt's shearing-stress formula, function of x and r in general, Equation (1), Part II

ρ = density of fluid in duct

Subscripts

avg = average

E = transport of energy

i = induced stream conditions in plane of nozzle

j = jet-stream conditions in plane of nozzle

x = conditions in cross section of flow at distance x from nozzle

o = conditions in plane of jet nozzle

∞ = condition that would be obtained by complete mixing of the flow at any section with no further loss of momentum or energy

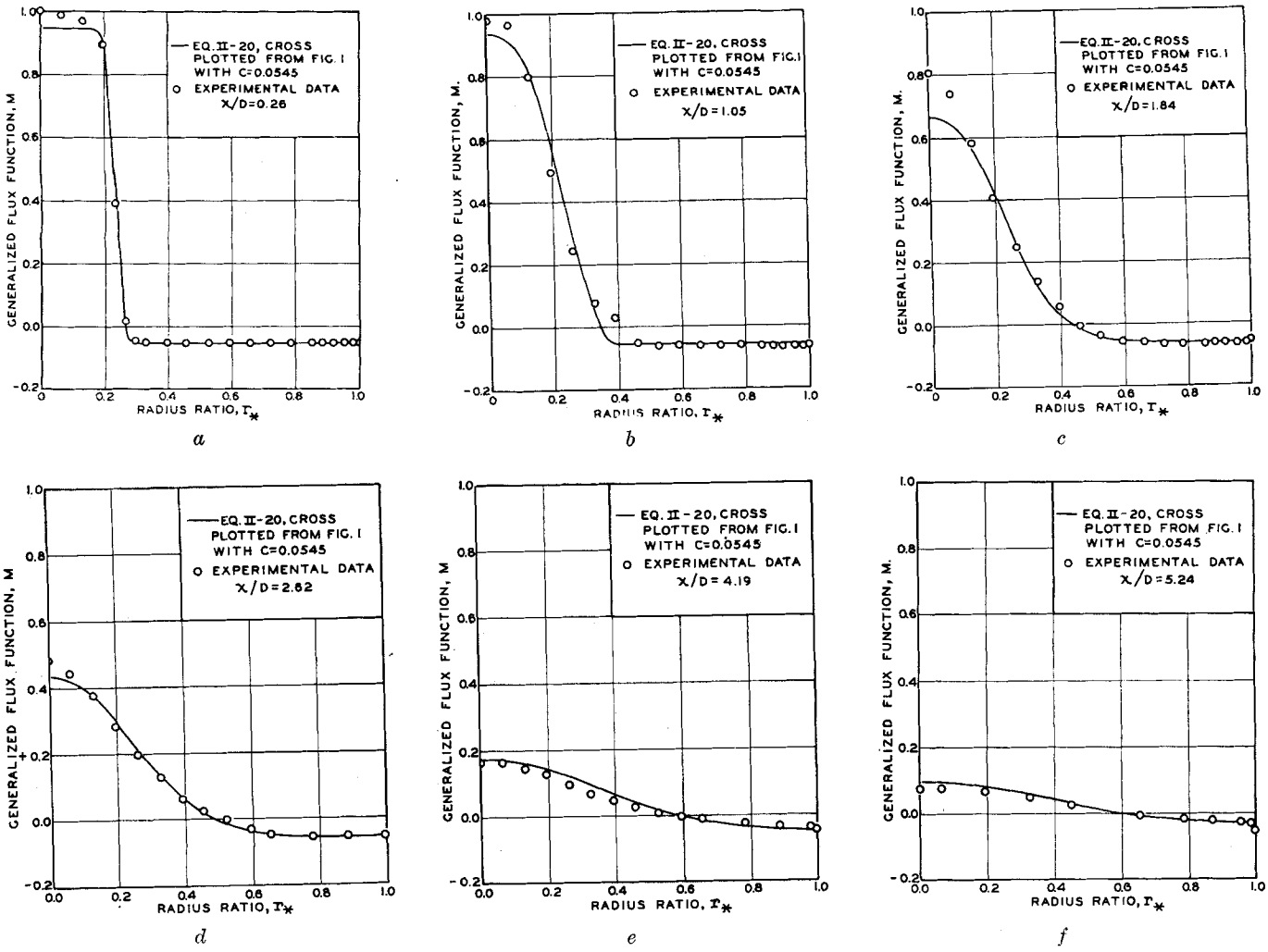

FIG. 4. CORRELATION OF GENERALIZED FLUX FUNCTION M FOR TRANSPORT OF ENERGY.

LITERATURE CITED

1. Alexander, L. G., E. W. Comings, H. L. Grimmett, and E. A. White, *Chem. Eng. Progr. Symposium Series* No. 10, **50**, 93 (1954).
2. Kivnick, A., Univ. Illinois Eng. Exp. Sta. Tech. Rept. 2, DA-18-064-CML-445 (1952).
3. Wagner, F., Rept. ZWB/UM/Re /7602, Arado Aircraft Co., Brandenburg, Germany; C.A.D.O. Translation A.T.I.-20255, A.M.C. Trans. F-TS-2559-Re, Wright Field, Dayton, Ohio (1944).

(Presented at the A.I.Ch.E. Biloxi meeting)